ACS OMEGA

http://pubs.acs.org/journal/acsodf

Article

Anticancer and Neuroprotective Activities of Ethyl Acetate Fractions from *Morus macroura* Miq. Plant Organs with Ultraperformance Liquid Chromatography-Electrospray Ionization-Tandem Mass Spectrometry Profiling

Dalia Ibrahim Hamdan,* Samia Salah, Wafaa Hassan Badr Hassan, Mai Morsi, Heba Muhammed Ali Khalil,* Omar Abdel-hamed Ahmed-Farid, Riham Adel El-Shiekh, Manal AbdElaziz Nael, and Ahmed Mohamed Elissawy

Cite This: *ACS Omega* 2022, 7, 16013−16027

Read Online

ACCESS | Metrics & More | Article Recommendations | Supporting Information

ABSTRACT: Column chromatography afforded the isolation of seven secondary metabolites (1-(2,4,6-trihydroxy phenyl)-ethanone-4-*O*-*β*-D-glucopyranoside, naringenin-7-*O*-*β*-D-glucopyranoside, kaempferol-3-*O*-*α*-L-rhamnoside, kaempferol-3-*O*-*β*-D-glucopyranoside, quercetin-3-*O*-*β*-D-glucopyranoside, quercetin-3-*O*-*β*-D-galactopyranoside, rutin) from the ethyl acetate (ET) fractions of *Morus macroura* Miq. stems (S), leaves (L), and fruits (F). Their identification based on ultraviolet (UV), electron ionization (EI), electrospray ionization-mass spectrometry (ESI-MS), and 1D and 2D NMR data. In addition, profiling of ET fractions using ultraperformance liquid chromatography-electrospray ionization-tandem mass spectrometry (UPLC-ESI-MS/MS) resulted in the identification of 82 compounds belonging to different classes, mainly polyphenolic constituents. Chemical profiling as well as molecular docking directed us to biological evaluation. Interestingly, the ET-L fraction exhibited a robust cytotoxic activity against HepG-2, MCF-7, and HELA cell lines. Also, it displayed a neuromodulatory activity against cisplatin neurotoxicity in rats by ameliorating the neurobehavioral dysfunction visualized in the open field and Y-maze test and modulating the neurochemical parameters such as brain amino acid levels (glutamate, aspartate, serine, and histidine), oxidative stress markers (GSH, MDA, and 8-hydroxy-2′-deoxyguanosine), and purinergic cell energy (adenosine triphosphate (ATP) and adenosine monophosphate (AMP)). In conclusion, the isolated compounds (kaempferol-3-*O*-*β*-glucoside and quercetin-3-*O*-*β*-glucoside) from the ET-L fraction could serve as potent anticancer agents due to their strong antioxidant, *in vitro* cytotoxicity, and *in vivo* neuroprotective activity.

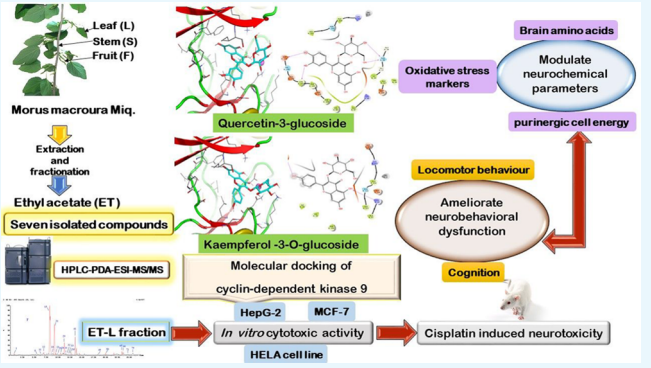

1. INTRODUCTION

The genus *Morus* family *Moraceae* includes 40 genera and 1000 species of monoecious rarely dioecious plants distributed in tropical and subtropical regions.[1] This genus is famous for the biosynthesis of bioactive metabolites such as Diels−Alder type adducts, phenolic acids, flavonoid aglycone, prenylated flavonoids, flavonoid glycosides, anthocyanins, 2-arylbenzofurans, alkaloids, stilbenes, steroids, and triterpenoids.[2,3] Moreover, plants belonging to this genus had exhibited many significant biological activities such as antidiabetic, anticancer, antioxidant, anti-inflammatory, antimicrobial, antihyperlipidemic, and antihypertensive activities.[4] An up to date survey revealed the presence of a few reports about the isolation and identification of bioactive metabolites from *M. macroura* Miq, vice Diels−Alder type adducts such as guangsangons F, G, H, I, J, mulberrofuran J, and kuwanon J,[5] stilbene dimer as andalasin A,[6] triterpenoids such as *α*-amyrin acetate, 3-*β*-hydroxylup-20(29)-en-28-oic acid, 3-*β*-hydroxylup-12-en-28-oic acid, and butyrospermol acetate[7] and arylbenzofuran derivatives including moracins.[8]

Cancer is the most predominant cause of high mortality globally after cardiovascular diseases.[9] The incidence is usually increasing in middle and low-income countries.[10] There are many cancer treatment varieties, such as surgical interventions, radiotherapy, and/or chemotherapy. Cisplatin (*cis*-diammine-dichloroplatinum II), one of the platinum chemotherapeutic

Received: February 25, 2022
Accepted: April 13, 2022
Published: April 29, 2022

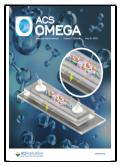

drugs, is used heavily to treat many cancers.[11] Despite its potent antitumor efficacy, it has many side effects that negatively affect cancer patients' health and quality of life.[12] Neurotoxicity is one of these side effects that occurred due to the ability of cisplatin to cross the blood-brain barrier (BBB) and induce weakness in the mature neurons of the brain.[13] It is manifested by many symptoms like locomotion incoordination, ototoxicity, and encephalopathy.[14] The prevalence of neurotoxicity increases with increasing the cumulative cisplatin dose above 300 mg/m^2 or 500 mg/m^2.[15]

Recent strategies recommend using pain killers or natural antioxidants along with cisplatin medication to reduce its side effects.[16] A considerable amount of studies has been published on the neuroprotectant effect of some herbal plants against cisplatin-induced neurotoxicity in rats like *Ginkgo biloba*,[17] *Azadirachta indica*,[18] and *Polygonum minus*.[19] However, no study was conducted on the *M. macroura* Miq and their role in protecting the brain against cisplatin neurotoxicity. Therefore, in our current study, we aimed to investigate the neuroprotectant activity of the ET-L fraction from *M. macroura* Miq against cisplatin-induced neurotoxicity in rats using behavioral and neurochemical assays. Besides, phytochemical investigations of the ET-L, ET-S, and ET-F fractions is done through UPLC-ESI-MS/MS profiling and other techniques used for secondary metabolites isolation.

2. EXPERIMENTAL SECTION

2.1. Plant Material. Fresh plant was gathered from a private nursery in Belbis in May 2014 and was kindly identified by Prof. Dr. Abdelhalem Abdelmogali, taxonomy researcher, Ministry of Agriculture, Dokki-Cairo, Egypt. A voucher specimen (MM100) was preserved in the herbarium of the Pharmacognosy Department, Faculty of Pharmacy, University of Zagazig.

2.2. Extraction, Fractionation, And Metabolites Isolation. Dried powdered stems (3.5 kg), leaves (2.5 kg), and fruits (1.0 kg) of *M. macroura* Miq were separately macerated with 80% aqueous ethanol at room temperature. The total ethanolic extracts of different plant organs were concentrated using a Buchi rotary evaporator (236, 704, and 86 g, respectively) and subsequently partitioned against light petroleum followed by dichloromethane and ethyl acetate (ET). Aliquots of the ET soluble fractions of different organs (5 g of the stem, 10 g of leaves, and 2.5 g of fruit) were separately subjected to silica gel column chromatography packed with methylene chloride, and the polarity of the mobile phase was gradually increased using methanol. The isolated pure compounds (Scheme S1) were subjected to an ESI-MS spectral analysis triple quadruple instrument (XEVO TQD), and acetonitrile−H_2O (1:5) was used as a matrix. In addition, ^{1}H NMR and ^{13}C NMR spectral analyses were recorded on a Bruker instrument (Switzerland) at 400 and 100 MHz, respectively, using CD_3OD as the solvent.

2.3. UPLC-ESI-MS-MS Analysis. ET fractions were subjected to UPLC-ESI-MS/MS analysis using negative and positive ion acquisition modes on a triple quadruple instrument (XEVO TQD, Waters Corporation, Milford, MA) mass spectrometer; column: ACQUITY UPLC-BEH C18 1.7 μm × 2.1 mm × 50 mm column. The samples were injected automatically using a Waters ACQUITY FTN autosampler. The mobile phase was filtered using a 0.2 μm filter membrane disc and degassed by sonication before injection. Its flow rate was 0.2 mL/min using a gradient mobile phase (methanol and water acidified with 0.1% formic acid that applied from 10% to 30% in 5 min, then from 30% to 70% in 10 min, then from 70% to 90% in 5 min, then holds the gradient for 3 min, then from 90% to 10% in 3 min). The instrument was controlled by Masslynx 4.1 software.

2.4. *In Vitro* Evaluation. *2.4.1. Cytotoxic Activity.* The tested samples (ET-L, ET-S, and ET-F) were investigated at different concentrations (500, 250, 125, 62.5, 31.25, 15.6, 7.8, and 3.9 μg/mL) against breast carcinoma (MCF-7), cervical carcinoma (HELA), and liver carcinoma (HepG-2) cell lines that were obtained from the Faculty of Pharmacy, Pharmacology Department, Al-Azhar University and maintained in Dulbecco's modified Eagle's medium (DMEM). Also, quercetin-3-*O*-β-D-glucopyranoside and kaempferol-3-*O*-β-D-glucopyranoside, isolated from ET-L, were investigated against the HELA cell line seeded in 96-well plates (10 000 cells per well in 100 μL of growth medium). According to published protocols, cells were fixed and stained for 10 days.[20] Optical density readings were carried out at 490 nm using a microplate reader (SunRise, TECAN, Inc., USA) to determine the percentage of viability.

2.4.2. Antioxidant Activity. DPPH (2,2-diphenyl-1-picrylhydrazyl) was used to evaluate the antioxidant activity of ET-S, ET-L, and ET-F fractions at different concentrations according to Rice-Evans, Halliwell, Lunt, and Halliwell.[21] Additionally, methanol solution (40 mL) of tested samples were added to 3 mL of methanolic solution of freshly prepared DPPH radicals (0.004% w/v) according to Yen and Duh.[22] The absorbance of the tested samples, control, and ascorbic acid as a reference standard were measured at λ_{max} 517 nm. The percentage of DPPH radical scavenging was calculated depending upon the following formula:

$$\%\text{antioxidant activity (E)} = [A_c - A_t)/A_c] \times 100$$

, where A_c is the absorbance of methanol solution of DPPH and A_t is the absorbance of the extracted sample with DPPH.

2.5. Molecular Docking. Cyclin-Dependent Kinase 9 (CDK9) was selected for docking. The protein structural file of the human CDK9/cyclinT1 in complex with Flavopiridol (PDB accession code 3BLR) was downloaded from the protein data bank repository (www.rcsb.org). The protein structure was prepared for docking by adjusting the bond orders, adding missing hydrogen atoms, filling in missing side chains and loops with prime, and deleting artificial water molecules. Although it does not affect the docking simulation, we kept cyclinT1. The hydrogen bond network was assigned by sampling water orientations and adjusting the protonation states of the amino acids. Restrained energy minimization was carried out using OPLS3e to remove atomic clashes. ATP atomic coordinates were selected to define the receptor grid for docking. To impart some degree of flexibility during the docking process, we modified the van der Waals radius scaling factor to 0.85 with a partial charge cutoff of 0.25. This will allow the ligand to use more space for docking. We allowed the rotation of receptor hydroxyl and thiol groups to simulate the actual ligand fitting. The 3D structures of the compounds were downloaded from PubChem (pubchem.ncbi.nlm.nih.gov). All acceptable protonation and tautomerization states were generated at pH 7.4 using LigPrep. After ligand preparation, we run the docking simulation using Glide SP (Standard precision). The ligand was treated as flexible, and the receptor was considered rigid with softened potentials.

https://doi.org/10.1021/acsomega.2c01148
ACS Omega 2022, 7, 16013−16027

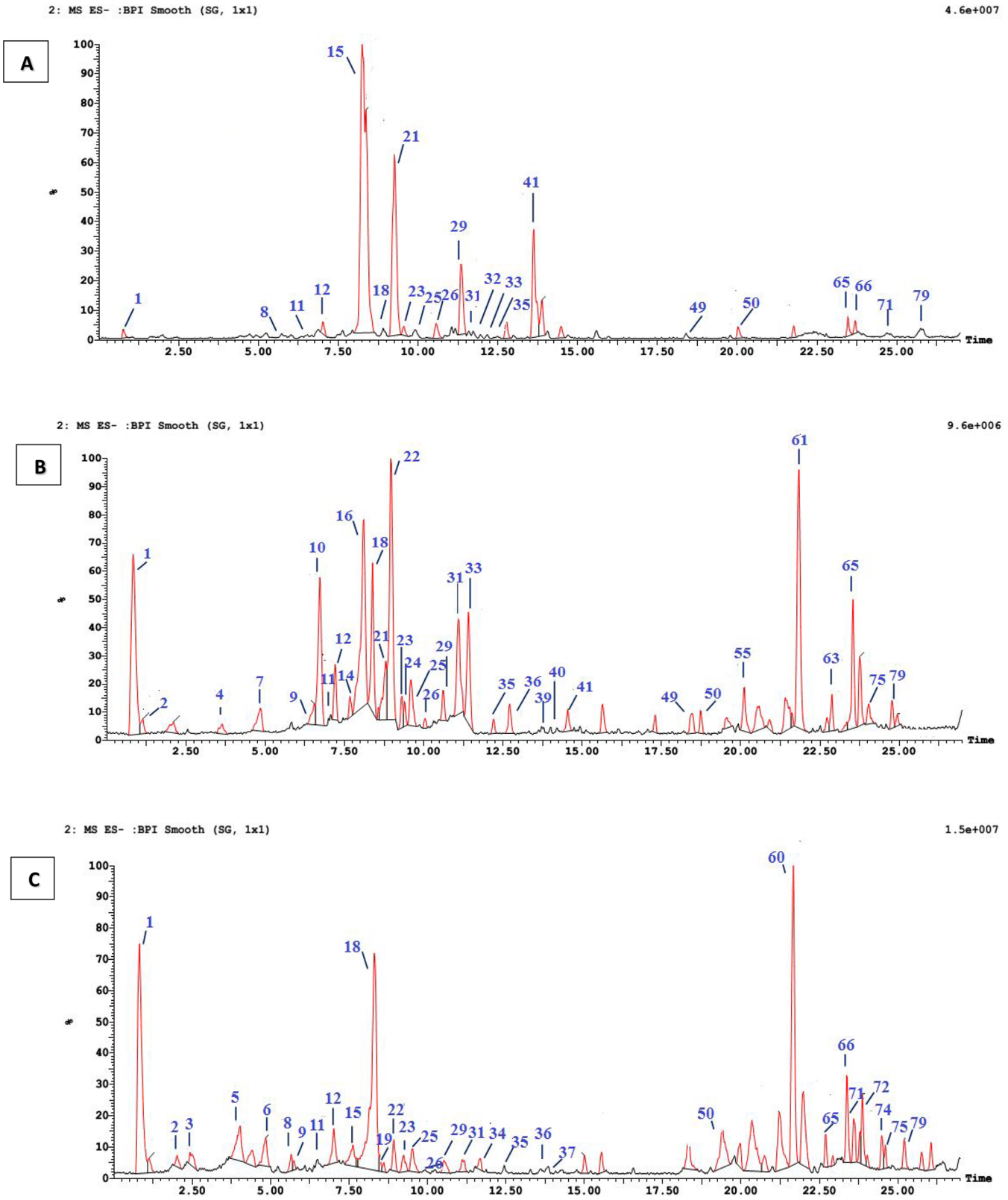

Figure 1. UPLC-ESI-MS/MS chromatograms (negative mode) of ET-L (A), ET-S (B), and ET-F (C) fractions of *M. macroura*, ET-L: ethyl acetate fractions of leaves; ET-S: ethyl acetate fractions of stems; ET-F: ethyl acetate fractions of fruits.

2.6. *In Vivo* Evaluation. *2.6.1. Animals.* Twenty-eight male Wistar rats weighing between 100−120 g were purchased from a commercial animal house (Giza, Egypt). They were maintained at standard environmental conditions and fed with commercial rodent ration and water ad libitum. All the experimental procedures agreed with the National Institutes of Health Guide for the Care and Use of Laboratory Animals (NIH Publications No. 8023, revised 1978). They were approved by the Veterinary Institutional Animal Care and Use Committee (VET-IACUC: Approval Number, Vet CU28/04/

https://doi.org/10.1021/acsomega.2c01148
ACS Omega 2022, 7, 16013−16027

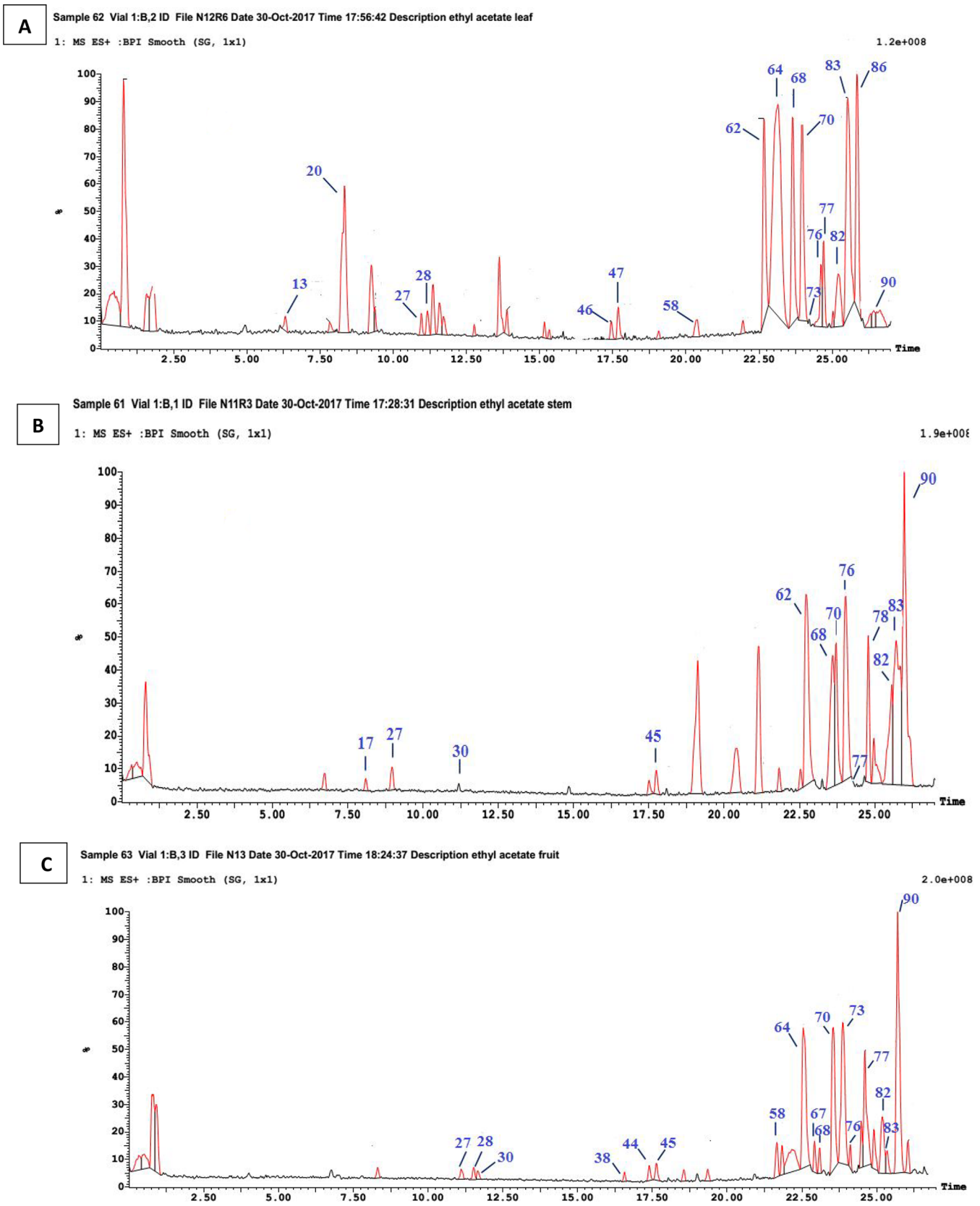

Figure 2. UPLC-ESI-MS/MS chromatograms (positive mode) of ET-L (A), ET-S (B), and ET-F (C) fractions of *M. macroura*, ET-L: ethyl acetate fractions of leaves; ET-S: ethyl acetate fractions of stems; ET-F: ethyl acetate fractions of fruits.

2021/269) of the Faculty of Veterinary Medicine, Cairo University.

2.6.2. Experimental Design. Animals were randomly divided into four groups of seven animals each, as follows: Group I: control, rats were administrated 2 mL/kg distilled

https://doi.org/10.1021/acsomega.2c01148
ACS Omega 2022, 7, 16013−16027

Table 1. Compounds Identified in the Ethylacetate Fractions of Leaves (ET-L), Stems (ET-S), and Fruits (ET-F) of *M. macroura* Miq by Using UHPLC-ESI/MS/MS in Positive and/or Negative Ionization Modes

peak no.	RT	RRT	MS $^{1-/+}$	MS^2	leaves	stems	fruits	tentative assignment	refs
1	0.82	0.032	353/−	191(100%) 179 (15%)	0.59	10.47	14.98	chlorogenic acid	33
2	2.1	0.084	153/−	109		0.74		protocatecheic acid	34
3	2.43	0.097	339/−	177 (100%)			0.82	aesculin	35
4	3.63	0.145	137/−	93 (100%)		0.57		hydroxybenzoic acid	36
5	3.86	0.155	353/−	191 (100%) 179 (32%)			2.76	neochlorogenic acid	
6	4.84	0.194	353/−	173 (100%) 179 (90%)			1.7	cryptochlorogenic acid	33
7	4.84	0.194	137/−	93 (100%)		0.57		hydroxybenzoic acid isomer	36
8	6.27	0.251	339/−	177, 175, 161, 135, 109	0.39		0.77	morachalcone A	37
9	6.27	0.251	431/−	269 (100%)		2.71	0.31	apigenin-7-*O*-*β*-glucoside	38
10	6.73	0.269	163/−	119 (100%)		6.66		coumaric acid	36
11	6.92	0.277	463/−	270.7	0.85	0.61	0.31	naringenin derivatives	39
12	7.26	0.291	447/−	285, 256.9, 242.5, 198.8	0.36	0.61	1.22	luteolin-7-*O*- glucoside	38
13	7.46	0.299	−/355	193	0.29			scopolin	40
14	7.62	0.305	431/−	341, 311, 269		0.61		vitexin (apigenin-8-*C*-glucoside)	39
15	7.92	0.317	463/−	301, 257			0.88	morin-*O*-*β*-glucoside	41
16	8.05	0.323	667/−	6, 49, 407		1.02		3-hydroxy kuwanol E	42
17	8.1	0.325	−/449	287		0.35		cyanidin-3-*O*-glucoside	43
18	8.25	0.331	463/−	301 (100%)	50.85	10.91	√	[a]quercetin-3-*O*-*β*-D-glucoside (**isoquercitrin**)	35
19	8.3	0.333	609/−	463, 301			17.63	[a]rutin	44
20	8.32	0.333	−/949	717, 465, 303 (100%) from MS 1	6.61			delphinidin derivative	45
21	8.38	0.336	463/−	301	√	4.93		[a]quercetin-3-*O*-*β*-galactoside (**hyperoside**)	46
22	8.53	0.342	431/−	285, 284, 255, 227		0.2		kaempferol-3-*O*-*β*- rhamnoside (**afzelin**)	47
23	8.71	0.349	447/−	269	0.71	0.95	1.22	apigenin-7-*O*-glucuronide	48
24	8.96	0.359	431/−	269		11.38		apigenin-7-*O*- glucoside isomer	38
25	9.24	0.37	447/−	285	20.63	0.95	0.88	[a]kaempferol-3-*O*-*β*-glucoside (**astragalin**)	35
26	9.24	0.37	447/−	343, 301	0.71	0.95	0.88	quercetin-8-*C*-rhamnoside	33
27	10.95	0.439	−/611	303, 328	18.93	7.53	4.54	hesperidin	49
28	10.95	0.439	−/610	317.5, 256.8, 151.2	0.46		0.99	petunidin dirhamnoside	50
29	11.14	0.446	447/−	301, 255	0.71	1.95	0.88	quercetin-3-*O*-*β*- rhamnoside (**quercitrin**)	33
30	11.18	0.448	−/397	351		1.35		unknown	
31	11.34	0.454	301/−	139 (100%), 256	1.3	0.43	0.77	ellagic acid	35
32	11.34	0.454	355/−	193.3 (100%)			0.67	ferulic acid-*O*-glucoside	35
33	11.37	0.456	431/−	285, 284, 255, 227		1.43	0.3	kaempferol-3-*O*-*β*- rhamnoside isomer (**afzelin**)	33
34	11.49	0.46	285/−		6.33			kaempherol	51
35	12.1	0.485	301/−	179, 151, 121	1.3	0.43	0.77	quercetin	35
36	12.85	0.515	271/−	271, 58			1.5	moracin J	
37	12.17	0.488	301/−	256, 151, 107	1.42	4.92		morin	
38	13.39	0.537	−/535	255			0.48	unknown	
39	14.06	0.563	467/−	305		√		gallocatechin glycoside	35
40	14.15	0.567	467/−	305		√		epigallocatechin glycoside	
41	14.39	0.577	329/−	287 [M − H − $COCH_3$]	0.91	0.77		[a]phloracetophenone-4-*O*-glucoside	52
42	14.68	0.588	575/−			√		unknown	
43	16.04	0.643	467/−			√		unknown	
44	17.23	0.691	−/343				1.2	unknown	
45	17.77	0.712	−/579			0.48	0.91	unknown	
46	17.83	0.715	−/355	203	0.86			epoxybergamottin	53
47	17.83	0.715	−/355	299, 69	0.29			albanin A	54
48	18.38	0.737	293/−	220.8 (100%)		0.01		hydroxy octadecatrienoic acid	55
49	18.87	0.756	591/−	287	√	0.33		cyanidin cinnamoyl glucuronide	56
50	19.77	0.792	317/−		0.86	1.73	1.05	unknown	
51	20.29	0.813	271/−	150.7 (100%)			√	naringenin	57
52	20.86	0.836	−/369				√	unknown	
53	21.08	0.845	475/−	299		0.05		chrysoeriol-uronic acid	38
54	21.1	0.846	−/355	177	0.29		1.29	sanggenon F	37

https://doi.org/10.1021/acsomega.2c01148
ACS Omega 2022, 7, 16013−16027

Table 1. continued

peak no.	RT	RRT	MS $^{1-/+}$	MS^2	leaves	stems	fruits	tentative assignment	refs
55	21.4	0.858	433/−	271		2.14		[a]naringenin-7-*O*-*β*-glucoside	58
56	21.49	0.861	−/381	318, 163, 71, 69	√			brasicasterol	59
57	21.74	0.871	475/−	410.9, 299.0	√			diosmetin glucuronide	60
58	21.99	0.881	475/−	255			0.01	palmitic acid ester	61
59	22.03	0.883	−/427	363.5			√	lupeol	62
60	22.06	0.884	423/−				4.5	unknown	
61	22.51	0.902	279/−			1.02		unknown	
62	22.73	0.911	−/683	331	6.65	3.9		malvidin diglucoronide	63
63	23.02	0.922	451/−	249.8, 390.5, 406.7, 435.1		1.73		melissic acid	64
64	23.06	0.924	−/683	597, 435, 287	5.4		√	cyanidin derivative	65
65	23.24	0.931	255/−		√	3.86	√	unknown	
66	23.47	0.941	281/−		√		1.71	unknown	
67	23.55	0.944	−/391	279, 149 (100%)			10.77	bis(2-ethyl hexyl) phthalate	66
68	23.6	0.946	−/611	302, 328, 229, 201	4.46	7.53	4.54	peonidin rutinoside	67
69	23.67	0.949	−/663	301	√			peonidin derivative	68
70	23.72	0.951	−/593	287, 434, 595	0.43	5.18	0.81	cyanidin rutinoside	69
71	23.83	0.955	349/−		0.68		0.8	unknown	
72	23.86	0.956	395/−	281			2.31	oleic acid ester	70
73	24.14	0.967	−/607	286	6.4		1.75	australisine A	71
74	24.44	0.979	283/−	239 [M − H − COO]			√	octadecanoic acid	72
75	24.45	0.981	339/−	162.9		0.33	1.09	coumaric acid glucuronide	38
76	24.65	0.988	−/535	317, 153	6.99	15.18	0.61	isorhamnetin-3-*O*-acetyl glucuronide	73
77	24.65	0.988	−/536	317, 153	0.99	15.18	0.61	petunidin 3-*O*-acetyl glucuronide	74
78	24.78	0.993	−/463	301		4.37		peonidin glucoside	75
79	24.95	1	339/	163 (100%)	0.71	0.78	13.61	euchrenone a7	76
82	25.53	1.023	−/683	597 (loss of 86), 435 (loss of glucose), 287.7	10.15	12.42	4.39	cyanidin-3-*O*-malonyl glucoside derivative	77
83	25.84	1.035	−/535	287	6.99	15.18	17.51	cyanidin-3-*O*-malonyl glucoside	77
90	27.68	1.109	−/398	314	6.4	9.35	1.31	24-methylene-ergosta-5-en-3*β*-ol	75

[a]Compounds isolated as pure compounds from *M. macroura* Miq are listed in bold. √ denotes that compounds are minor.

water daily. Group II: cisplatin (Mylan, The Netherlands) at a single dose 10 mg/kg body weight, i.p. Group III: ET-L200, 200 mg/kg body weight ET-L fraction gavaged daily for 15 days. Group IV: cisplatin + ET-L200, 200 mg/kg body weight ET-L fraction gavaged daily for 15 days + cisplatin 10 mg/kg body weight, i.p. as a single dose. Cisplatin administration was performed on the tenth day of the experiment, 1 h after administration of ET-L200. The dosage of cisplatin was selected according to previous studies,[23] while the dose of the ET-L fraction was selected according to a previous study.[24]

2.6.3. Behavioral Testing. At a time 24 h after the last dose of ET-L200, rats were submitted to open field testing and the Y-maze to assess the locomotor behavior and working memory. The behavioral tests were performed as previously mentioned.[25,26] The measuring parameters for the open field test were the number of crossing squares and rearing activity which were recorded for 3 min. However, the number of arm entries and spontaneous alternation percentage (SAP%) were evaluated for 5 min as working memory indicators in the Y-maze test. After the last behavioral test, all rats were euthanized by cervical dislocation, and the brains were excised gently and preserved at −80 °C for further neurochemical analyses.

2.6.4. Neurochemical Analyses. HPLC is a convenient method used for the detection of several neurochemicals, where the level of glutamate in the brain was detected according to Heinrikson et al.,[27] while brain monoamines levels were measured according to Pagel et al.[28] Oxidative stress markers (reduced glutathione (GSH), malondialdehyde (MDA), and 8-hydroxy-2′-deoxyguanosine (8-OHdG)) were also measured according to Jayatilleke et al., Karatepe et al., and Lodovici et al.,[29−31] respectively. Concerning brain cell energy levels, adenosine triphosphate (ATP) and adenosine monophosphate (AMP) were determined according to Teerlink et al.[32]

2.6.5. Statistical Analysis. The *in vitro* studies were performed in triplicates. The *in vivo* study was analyzed using SPSS 24.0 software. ANOVA followed by Bonferroni post hoc analysis for multiple comparisons and Pearson correlation for neurochemical parameters were used for statistical analysis. Data were expressed means ± SEM, and significance was set at $P \leq 0.05$. Graphs were drawn using SPSS and Graph Pad Prism version 6.00.

3. RESULTS

3.1. Phytochemical Results. Column chromatography packed with different stationary phases in combination with semipreparative HPLC of the ET soluble fractions afforded the isolation and identification of seven metabolites, where compounds (**1**, **2**, **3**) isolated from ET-S, (**4**, **5**, **6**) from ET-L and (**7**) ET-F (Figures 1 and 2, Supplementary text sections ST1−ST7, Figure S1−S27, and Scheme S1).

3.2. Characterization of Secondary Metabolites Analyzed by UPLC -ESI-MS/MS. Phenolic and nonphenolic compounds were identified in the ET-L, ET-S, and ET-F fractions of *M. macroura* Miq by UPLC-ESI-MS/MS. The distribution of these compounds and their percentages are gathered in Table 1 and described in Supplementary text section ST8.

https://doi.org/10.1021/acsomega.2c01148
ACS Omega 2022, 7, 16013−16027

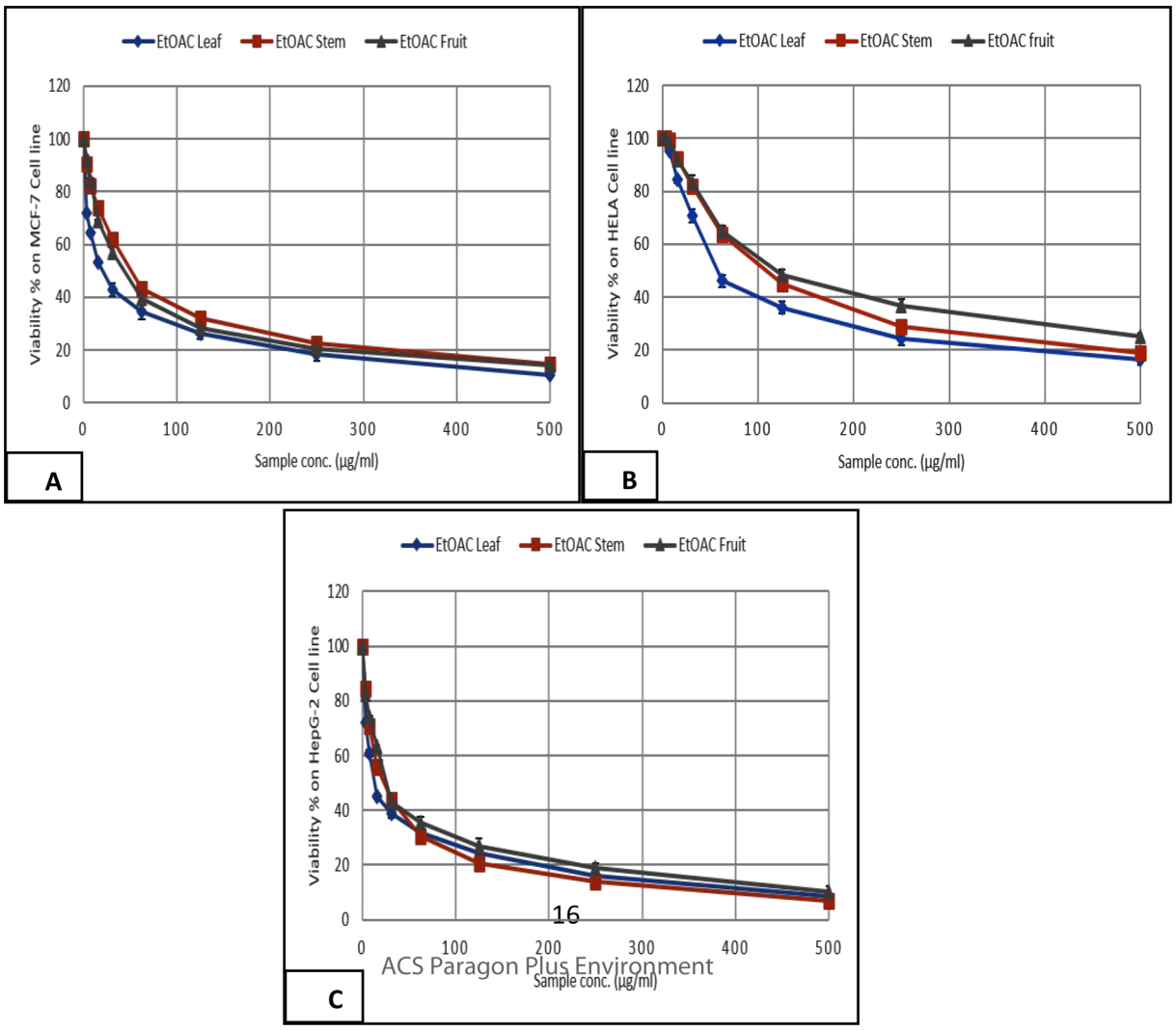

Figure 3. Effect of ethyl acetate fractions of leaves (ET-L), stems (ET-S) and fruits (ET-F) of *M. macroura* Miq. on the viability % MCF-7 (A), HELA (B), and HepG-2 (C) cell lines.

3.3. Biological Results. *3.3.1. In Vitro Cytotoxic Activity 2.* Different concentrations of ET fractions were evaluated against different tumor cells MCF, HELA, and HepG-2. The ET-L was the most active fraction against HepG-2 (13.2 μg/mL) and MCF-7 (20.5 μg/mL). Moreover, ET-S and ET-F showed moderate activity against HepG-2 (23.2 μg/mL and 25.8 μg/mL) and MCF-7 (51.0 μg/mL and 43.7 μg/mL), respectively (Figure S2). Additionally, quercetin-3-*O*-β-D-glucopyranoside and kaempferol-3-*O*-β-D-glucopyranoside exhibited strong and moderate activity against the HELA cell line with IC_{50} = 19.8 μg/mL and 61.4 μg/mL, respectively compared to doxorubicin (Figures 3−5).

3.3.2. In Vitro Antioxidant Activity. The DPPH scavenging percentage of ET fractions and ascorbic acid and SC_{50} values (the concentration required to scavenge DPPH by 50%) are shown in Figure S27. The ET-L fraction showed the highest antioxidant activities as indicated by their high SC_{50} followed by ET-F and ET-S fraction (SC_{50} 5.53 ± 0.04, 10.6 ± 0.02, and 44.2 ± 0.11, respectively) compared to ascorbic acid (SC_{50} 5.3 ± 0.04).

3.3.3. Molecular Docking. We selected CDK9 to investigate the expected mechanism of kaempferol-3-*O*-β-glucoside and quercetin-3-*O*-β-glucoside as anticancer agents. The results

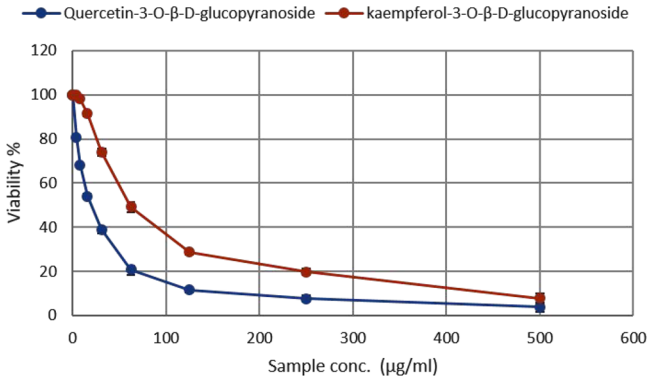

Figure 4. Effect of quercetin-3-*O*-glucoside and kaempferol-3-*O*-glucoside on the viability % HELA cell line.

showed that kaempferol-3-*O*-β-glucoside and quercetin-3-*O*-β-glucoside fit well within the binding site of CDK9 with binding energy values of −8.4 kcal/mol for quercetin-3-*O*-β-glucoside and −7.5 kcal/mol for kaempferol-3-*O*-β-glucoside compared to −9.1 kcal/mol for the reference compound (flavopiridol). The compounds showed a hydrogen bond to the hinge amino acid residues Cys 107 and Asp 110 and electrostatic

https://doi.org/10.1021/acsomega.2c01148
ACS Omega 2022, 7, 16013−16027

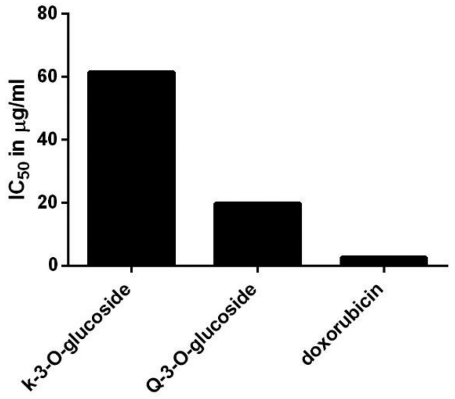

Figure 5. IC_{50} (μg/mL) of quercetin-3-*O*-glucoside, kaempferol-3-*O*-glucoside, and doxorubicin as standards against the HELA cell line.

interactions to the Mg^{2+} ion. These interactions are conserved in the native ligand's complexes. The conserved Lys residue (Lys 49) showed strong ion−cation interactions with the aromatic rings of these flavonoids. In general, the oxygen containing functionalities orient themselves in the proper position to face the hinge region allowing for forming the required hydrogen bonds (Figures 6 and 7).

3.3.4. In Vivo Evaluation. 3.3.4.1. Behavioral Testing. 3.3.4.1.1. Open Field Test. As shown in Figure 8A,B, the locomotor behavior as visualized by the number of crossing squares and rearing activity was markedly decreased in the cisplatin intoxicated rats compared to the control group. On the other hand, the rats treated with cisplatin + ET-L200 showed a significant increase in the locomotion compared to the cisplatin intoxicated rats. There was no significant difference between control rats and ET-L200 treated rats.

3.3.4.1.2. Y-Maze. As demonstrated in Figure 8C,D, the cisplatin intoxicated rats showed a marked decrease in the number of Y-maze arms entries and spontaneous alternation percentage compared to control rats. Rats treated with cisplatin + ET-L200 showed a substantial increase in the arm entry frequency and spontaneous alternation percentage compared to cisplatin intoxicated rats.

3.3.4.2. Biochemical Analyses. 3.3.4.2.1. Brain Amino Acid Level. As shown in Figure 9A−D, cisplatin intoxicated rats exhibited a significant increase in most brain amino acid levels (glutamate, aspartate, serine, and histidine) in comparison to the control and ET-L200 treated rats. On the other hand, cisplatin + ET-L200 treated rats displayed a marked decrease in the amino acids level (glutamate and histidine) in comparison to control ET-L200 treated rats. Interestingly, ET-L200 administration decreased aspartate and serine levels near the control in cisplatin + ET-L200 treated rats.

3.3.4.2.2. Brain Oxidative Stress Markers. As depicted in Figure 10A−C, cisplatin intoxicated rats displayed a substantial increase in the MDA and 8OHdG levels and a marked decrease in the GSH level compared to the control and ET-L200 treated rats. In contrast, cisplatin + ET-L200 treated rats showed a mid amelioration of oxidative stress markers and recovered near the control group.

3.3.4.2.3. Brain Cell Energy Level. Cisplatin intoxicated rats displayed a marked exhaust of ATP and accelerated the degradation resembling the AMP content compared to the control and ET-L200 treated rats (Figure 11A,B). The cisplatin + ET-L200 treated rats displayed a mild recovery for ATP and a complete recovery for the AMP content compared to the control and ET-L200 treated rats.

3.3.4.2.4. Correlation Matrix Parameters. Figure 12 and Table 2 showed a positive correlation for Glu against ASP, Ser, His, MDA, 8OHdG, and AMP and negative against GSH and ATP. Also, GSH presents a positive correlation against ATP and negative from Glu, ASP, Ser, HIS, MDA, 8OHdG, and AMP.

4. DISCUSSION

Traditional column chromatography and hyphenated HPLC techniques were applied for profiling the ET-L, ET-S, and ET-F, where eight secondary metabolites were isolated by column chromatography and purified by preparative TLC as well as crystallization. Additionally, UPLC-ESI-MS/MS profiling afforded the identification of altogether 82 compounds, where about half of the identified compounds are present for the first time in the family Moraceae, such as phenolic acid glycosides (ferulic acid-*O*-glucoside, phloracetophenone-4-*O*-glucoside, and coumaric acid glucuronide), flavonoid glycosides (apigenin-*O*-glucoside, its isomer, kaempferol-3-*O*-rhamnoside, its isomer, luteolin-7-*O*-glucoside apigenin glucuronide, hesperidin, morin-3-*O*-glucoside, chrysoeriol-uronic acid, naringenin-7-*O*-glucoside, diosmetin glucuronide, isorhamnetin 3-*O*-acetyl glucuronide), tannin compounds (gallocatechin glycoside, epigallocatechin glycoside). More-

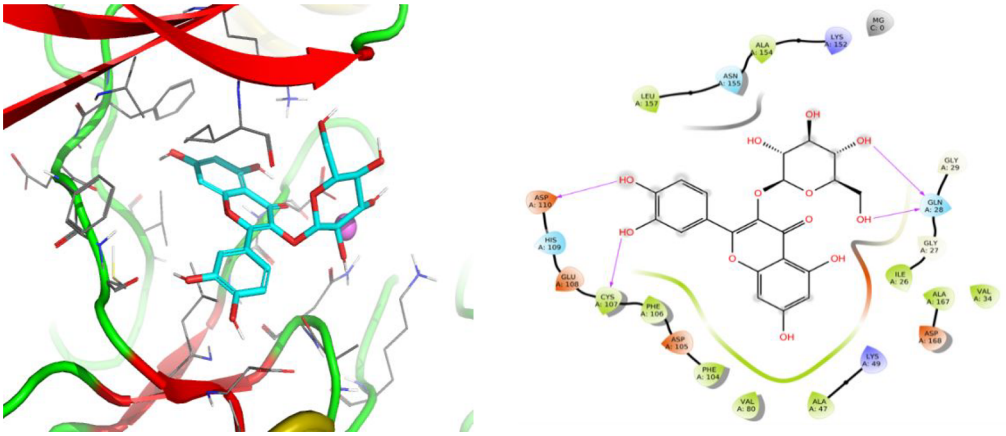

Figure 6. Interaction profile of quercetin-3-*O*-glucoside. (Left) 2D interaction map showing the interacting amino acids and the type of interaction. (Right) 3D figure of the protein−ligand complex showing the protein as a cartoon and the ligand as sticks. The Mg^{2+} is shown as a sphere.

https://doi.org/10.1021/acsomega.2c01148
ACS Omega 2022, 7, 16013−16027

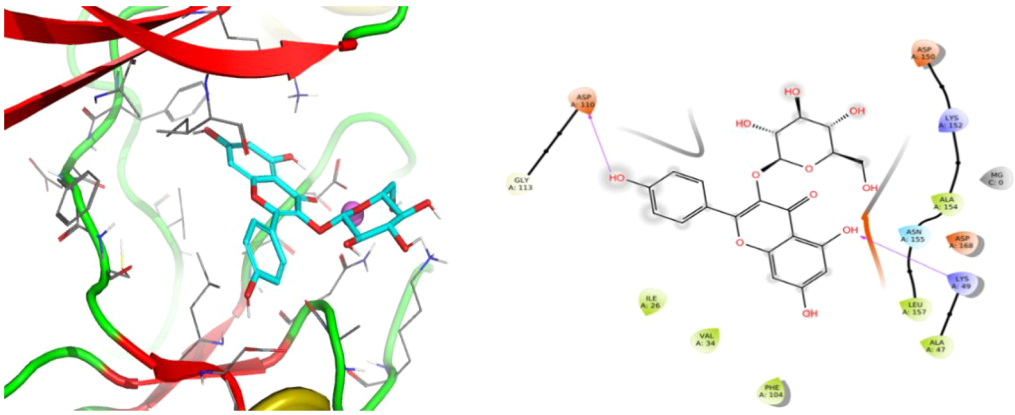

Figure 7. Interaction profile of kaempferol-3-*O*-glucoside. (Left) 2D interaction map showing the interacting amino acids and the type of interaction. (Right) 3D figure of the protein−ligand complex showing the protein as a cartoon and the ligand as sticks. The Mg^{2+} is shown as asphere.

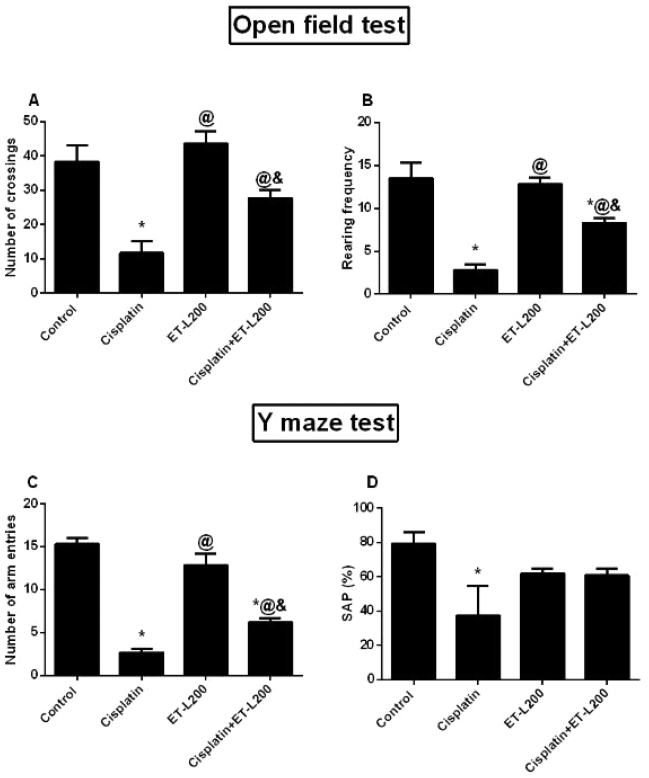

Figure 8. Effect of cisplatin and/or ET-L fraction of *M. macroura* on the locomotion and cognitive behavior of rats. (A) Open field test: number of crossings, (B) open field test: rearing frequency, (C) Y-maze: number of arm entries, and (D) Y-maze: spontaneous alternation percentage. Data are expressed as mean ± SEM, one-way ANOVA, followed by a post hoc test and Bonferroni test for seven rats in each group. *Significant from the control group, @ significant from the cisplatin group, &significant from the ET-L200 group. $p < 0.05$.

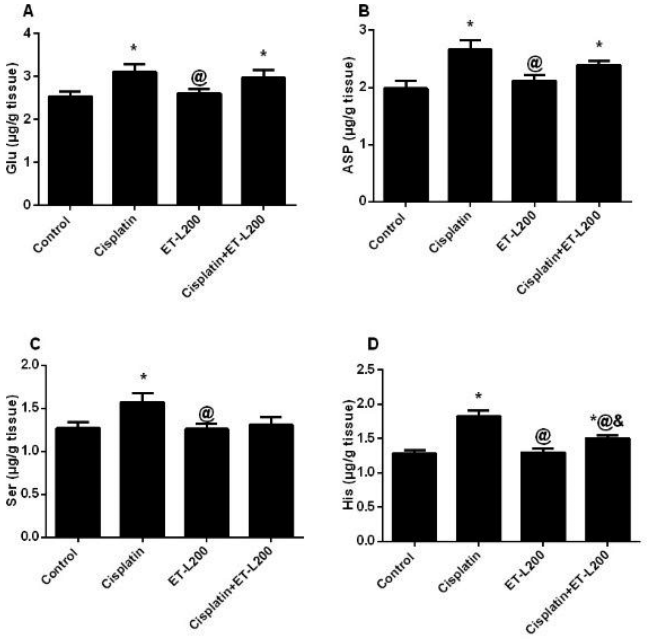

Figure 9. Effect of cisplatin and/or ET-L fraction of *M. macroura* on the brain amino acid levels of rats: (A) glutamate, (B) aspartate, (C) serine, and (D) histidine. Data are expressed as mean ± SEM, one-way ANOVA, followed by a post hoc test and Bonferroni test for seven rats in each group. *Significant from the control group, @ significant from the cisplatin group, &significant from the ET-L200 group. $p < 0.05$.

over, aesculin and epoxybergamottin are first reported in *Morus macroura* Miq. Also, anthocyanin derivatives such as compounds **20**, **28**, **49**, **62**, **64**, **69**, **77**, **78**, **82**, and **83** as well as melissic acids, steroids, and triterpenoids (cholesterol, brasicasteol, and 24-methylene ergosta-5-en-3β-ol) are first reported in *Morus macroura* Miq.

Furthermore, all the phenolic acids, compounds 3-hydroxy kuwanol E, moracin J, bis (2-ethylhexyl) phthalate, all flavonoid aglycones and glycosides, prenylated flavonoids, coumarins, all anthocyanins, fatty acids and their derivatives, all steroids and triterpenoids and their derivatives were identified for the first time in *Morus macroura* Miq. On top of these metabolites, quercetin-*O*-glucoside and kaempferol-*O*-glucoside, in a ratio of 50.85% and 20.63%, respectively, are the most abundant compounds in the ET-L fraction. In conclusion, *M. macroura* Miq. leaves exhibit higher contents of polyphenolics, and these findings are in agreement with that previously reported.[78]

In vitro cytotoxic and antioxidant activity of the ET-L, ET-S, and ET-F fractions were evaluated. The cytotoxic activity evaluation was based on IC_{50} values, according to Srisawat et al.[79] The ET-L fraction displayed the highest activity against HepG-2 and MCF-7 tumor cell lines. Also, they exhibited the

https://doi.org/10.1021/acsomega.2c01148
ACS Omega 2022, 7, 16013−16027

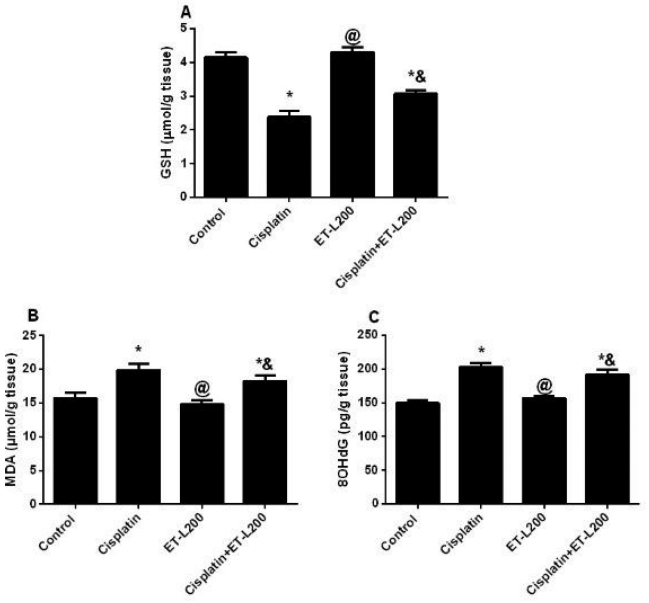

Figure 10. Effect of cisplatin and/or ET-L fraction of *M. macroura* on the oxidative stress markers of rats: (A) reduced glutathione, (B) malondaldhyde, and (C) 8-hydroxy-2′-deoxyguanosine. Data are expressed as mean ± SEM, one-way ANOVA, followed by a post hoc test and Bonferroni test for seven rats in each group. *Significant from the control group, @significant from the cisplatin group, &significant from the ET-L200 group. $p < 0.05$.

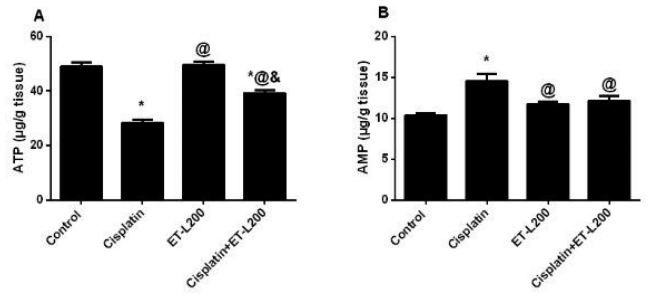

Figure 11. Effect of cisplatin and/or ET-L fraction of *M. macroura* on the brain cell energy level of rats: (A) adenosine triphosphate and (B) adenosine monophosphate. Data are expressed as mean ± SEM, one-way ANOVA, followed by a post hoc test and Bonferroni test for seven rats in each group. *Significant from the control group, @ significant from the cisplatin group, and &significant from the ET-L200 group. $p < 0.05$.

most increased antioxidant activity compared to ascorbic acid. These findings can be attributed to their high content of polyphenolics, especially quercetin-3-*O*-*β*-D-glucopyranoside and kaempferol-3-*O*-*β*-D-glucopyranoside.[78] They also showed potent cytotoxic activity against the HELA tumor cell line compared to doxorubicin.

In general, plant polyphenolics as free radical scavengers have attracted tremendous interest as possible natural therapeutics against free radical-mediated diseases such as atherosclerosis, cancer, asthma, diabetes, dementia, and inflammatory joint and degenerative eye diseases.[78,80] Therefore, based on the strong cytotoxic and antioxidant activity of the ET-L fraction, in vivo cisplatin-induced neurotoxicity was conducted on rats to further confirm the ET-L fraction cytotoxic and antioxidant activities against cisplatin.

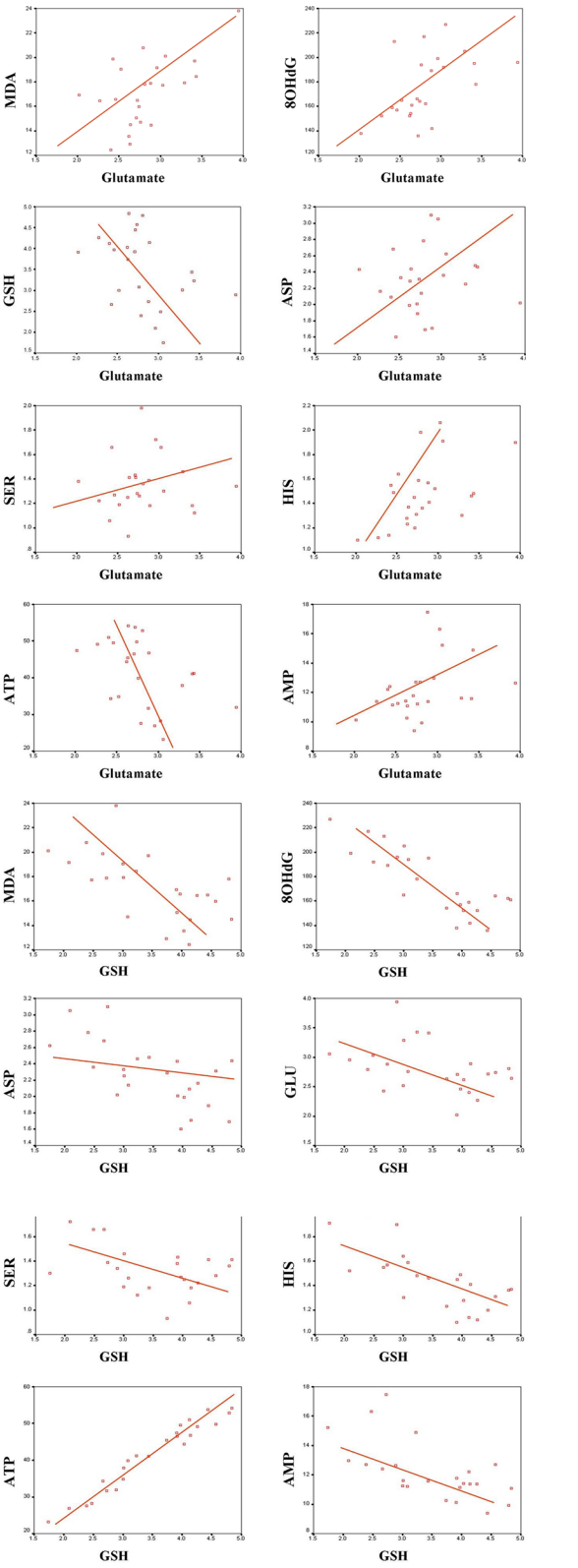

Figure 12. Scatter correlation matrixes against GLU and GSH and subsequent parameters.

Our in vivo results showed that single intraperitoneal administration of cisplatin (10 mg/kg) causes evident neurobehavioral and neurochemical changes. The neurobehavioral changes, including anxiety-like behavior, and the general activity is reduced in cisplatin intoxicated rats in the

https://doi.org/10.1021/acsomega.2c01148
ACS Omega 2022, 7, 16013−16027

Table 2. Correlation Matrix of Some Biochemical Parameters[a]

	Glu	GSH	ASP	Ser	His	MDA	8OHdG	ATP	AMP
Glu	ND	−0.388	0.089	0.04	0.507	0.562	0.51	−0.435	0.383
		0.061	0.678	0.853	0.011	0.004	0.011	0.034	0.065
GSH	−0.388	ND	−0.653	−0.448	−0.739	−0.624	−0.839	0.975	−0.633
	0.061		0.001	0.028	0	0.001	0	0	0.001
ASP	0.089	−0.653	ND	0.439	0.317	0.382	0.598	−0.656	0.591
	0.678	0.001		0.032	0.131	0.065	0.002	0	0.002
Ser	0.04	−0.448	0.439	ND	0.504	0.484	0.513	−0.494	0.24
	0.853	0.028	0.032		0.012	0.017	0.01	0.014	0.26
His	0.507	−0.739	0.317	0.504	ND	0.647	0.725	−0.805	0.601
	0.011	0	0.131	0.012		0.001	0	0	0.002
MDA	0.562	−0.624	0.382	0.484	0.647	ND	0.659	−0.667	0.341
	0.004	0.001	0.065	0.017	0.001		0	0	0.103
8OHdG	0.51	−0.839	0.598	0.513	0.725	0.659	ND	−0.836	0.568
	0.011	0	0.002	0.01	0	0		0	0.004
ATP	−0.435	0.975	−0.656	−0.494	−0.805	−0.667	−0.836	ND	−0.672
	0.034	0	0	0.014	0	0	0		0
AMP	0.383	−0.633	0.591	0.24	0.601	0.341	0.568	−0.672	ND
	0.065	0.001	0.002	0.26	0.002	0.103	0.004	0	

[a]0 to 0.3 (0 to −0.3) negligible correlation; 0.3−0.5 (−0.3 to −0.5) low positive (negative) correlation; 0.5−0.7 (−0.3 to −0.7) moderate positive (negative) correlation; 0.7−0.9 (−0.7 to −0.9) high positive (negative) correlation; 0.9−1 (−0.9 to −1) very high positive (negative) correlation.

open field test. The open field test is generally used to evaluate the anxiety-like behavior and the locomotor activity of rodents. These results agreed with previous studies.[23] Furthermore, cisplatin causes cognitive impairment, a condition known as chemobrain, as evidenced by a reduction in arm entries and spontaneous alternation percentages in the Y-maze. The Y-maze test is used to evaluate the working memory in rodents. These data agreed with those recorded in earlier studies.[81,82] However, the administration of the ET-L fraction was able to ameliorate most of the detrimental effects caused by cisplatin as evidenced by an increase in the general motor activity in the open field test and an increase in the arm entries and spontaneous alternating percentages in the Y-maze. Previous studies supported these findings that discussed the role of quercetin and kaempferol in ameliorating the behavioral dysfunction associated with lipopolysaccharide-induced neuroinflammation[83] and stressful events.[84]

A possible explanation for these behavioral dysfunction might be due to the disturbance in the glutamatergic system in the cisplatin intoxicated rats. Glutamate is one of the most excitatory neurotransmitters responsible for the common cognitive functions in the cerebral cortex.[85] It is worth noting that the secretion of a lot of glutamates leads to excitatory toxicity.[86] Glutamate oversecretion leads to the influx of calcium ions into the cell, leading to the activation of many enzymes, such as phospholipase, nuclease, and proteases such as calbin. These enzymes then destroy cell structures such as the cytoskeleton, the cell membrane, and DNA.[87] Downstream of glutamate overexpression leads to a negative correlation for GSH and ATP in which glutamate decrease GSH and purinergic cell energy remarked by ATP content. The glutamate-induced cytotoxicity is likely mediated through inhibition of cystine uptake through cystine/glutamate transporter inhibition leading to a depletion of cellular glutathione synthesis.[88,89] Glutathione played the main factor in the defense against oxidative stress; therefore, prolonged depletion of intracellular glutathione may lead to cell degeneration.

On the other hand, the administration of the ET-L fraction enhances the ROS scavenging properties accompanied by significantly lowering the lipid peroxidation status. This antioxidant property could be attributed to the presence of kaempferol and quercetin metabolites in the ET-L fraction.[90,91] Moreover, kaempferol ameliorates cell energy depletion, which may be the homeostasis's main causes via increasing mitochondrial ATP and decreasing turnover.[92] Also, it can indirectly reduce Ca^{2+} and regulate various Ca^{2+} subordinate enzymes (phospholipids, proteases, and nucleases), which leads to diminishing oxidative pressure and cell death.[93,94]

Additionally, cisplatin intoxicated rats exhibited elevated histidine and serine levels in the brain. Histidine is a precursor of brain histamine, responsible for maintaining the brain functions when releasing in an adequate amount. In contrast, histamine over secretion is associated with many disorders such as anxiety and appetite regulation.[95] In contrast, histidine showed amelioration level after the administration of the ET-L fraction which may depend on the anti-inflammatory and antihistaminic effects of quercetin.[96] In addition, serine is a nonessential amino acid in the body necessary for tumor cell survival.[97] The antitumor role of cisplatin exists in the reduction of phosphoglycerate dehydrogenase (PHGDH) and converts approximately 3-phosphoglyceric acid produced at glycolysis to 3-phosphatedehydropyruvate, which is a precursor of serine.[98] This conversion increases serine accumulation and increases the inhibitory amino acids. However, the administration of ET-L fraction may decrease the serine level. This may be attributed to its quercetin content as confirmed by ref 99 who found that quercetin can reduce the serine level via the Drp1 phosphorylation inhibited at serine 616 in cultured endothelial cells.

5. CONCLUSION

The high contents of phenolic compounds in the extract support their potent antioxidant and *in vitro* cytotoxic activity. The expected mechanisms of action of kaempferol-3-*O*-*β*-glucoside and quercetin-3-*O*-*β*-glucoside as anticancer agents is CDK9 inhibition. Moreover, The ET-L fraction modulated the neurobehavioral and neurochemical deficits associated with cisplatin in rats. As it increases the locomotor and cognitive

https://doi.org/10.1021/acsomega.2c01148
ACS Omega 2022, 7, 16013−16027

behavior visualized by an increase in the number of crossing squares and rearing activity in the open field test and the number of arm entries and spontaneous alternation percentage in the Y-maze test. Moreover, it moderates the brain amino acid levels (glutamate, aspartate, serotonin, and histamine), oxidative stress markers (GSH, MDA, and 8-hydroxy-2′-deoxyguanosine), and purinergic cell energy (ATP and AMP). All of these results render the ET-L fraction a promising candidate in the treatment of various types of cancer or even as a supplementary agent in cisplatin-treated patients.

■ ASSOCIATED CONTENT

Supporting Information

The Supporting Information is available free of charge at https://pubs.acs.org/doi/10.1021/acsomega.2c01148.

Supplementary text of compounds **1**, **2**, **3**, **4**, **5**, **6**, and **7**; characterization of secondary metabolites analyzed by UPLC-ESI-MS/MS; ESI-MS spectrum of compound **1** (Figure S 1), ^{1}H NMR spectrum of compound **1** (Figure S 2), APT spectrum of compound **1** (Figure S 3), HMBC correlations of compound **1** (Figure S 4), ESI-MS spectrum (positive mode) of compound **2** (Figure S 5), ^{1}H NMR spectrum of compound **2** (Figure S 6), APT spectrum of compound **2** (Figure S 7), HMBC correlations of compound **2** (Figure S 8), ESI-MS spectrum of compound **3** (Figure S 9), ^{1}H NMR spectrum of compound **3** (Figure S 10), APT spectrum of compound **3** (Figure S 11), ESI-MS spectrum of compound **4** (Figure S 12), ^{1}H NMR spectrum of compound **4** (Figure S 13), APT spectrum of compound **4** (Figure S 14), HMBC correlations of compound **4** (Figure S 15), ESI-MS spectrum of compound **5** (Figure S 16), ^{1}H NMR spectrum of compound **5** (Figure S 17), APT spectrum of compound **5** (Figure S 18), HMBC correlations of compound **5** (Figure S 19), ESI-MS spectrum of compound **6** (Figure S 20), ^{1}H NMR spectrum of compound **6** (Figure S 21), APT spectrum of compound **6** (Figure S 22), ESI-MS spectrum of compound **7** (Figure S 23), ^{1}H NMR spectrum of compound **7** (Figure S 24), APT spectrum of compound **7** (Figure S 25), chemical structure of isolated metabolites with HMBC of compound **1** (Figure S 26), DPPH scavenging capacity (SC_{50}) of ethyl acetate fractions of leaves (ET-L), stems (ET-S), and fruits (ET-F) of *M. macroura* Miq. and ascorbic acid at a concentration of 100 μg/mL (Figure S27); and Supplementary Scheme S 1, isolation of secondary metabolites from ethyl acetate fractions by column chromatography (PDF)

■ AUTHOR INFORMATION

Corresponding Authors

Dalia Ibrahim Hamdan − *Department of Pharmacognosy, Faculty of Pharmacy Menoufia University, Shibin Elkom 32511, Egypt*; Phone: +201289699978; Email: dalia1973@phrm.menofia.edu.eg

Heba Muhammed Ali Khalil − *Department of Veterinary Hygiene and Management, Faculty of Veterinary Medicine, Cairo University, Giza 12211, Egypt*; orcid.org/0000-0001-6008-2157; Phone: +201013666331; Email: heba.ali@cu.edu.eg

Authors

Samia Salah − *Department of Pharmacognosy, Faculty of Pharmacy, Zagazig University, Zagazig 44519, Egypt*

Wafaa Hassan Badr Hassan − *Department of Pharmacognosy, Faculty of Pharmacy, Zagazig University, Zagazig 44519, Egypt*

Mai Morsi − *Department of Pharmacognosy, Faculty of Pharmacy, Zagazig University, Zagazig 44519, Egypt*

Omar Abdel-hamed Ahmed-Farid − *Department of Physiology, National Organization for Drug Control and Research, Giza 12553, Egypt*

Riham Adel El-Shiekh − *Department of Pharmacognosy, Faculty of Pharmacy, Cairo University, Cairo 11562, Egypt*; orcid.org/0000-0002-3179-3352

Manal AbdElaziz Nael − *Department of Pharmaceutical Chemistry, Faculty of Pharmacy, Tanta University, Tanta 31527, Egypt*

Ahmed Mohamed Elissawy − *Pharmacognosy Department, Faculty of Pharmacy, Ain Shams University, Abbassia, Cairo 11566, Egypt*

Complete contact information is available at: https://pubs.acs.org/10.1021/acsomega.2c01148

Author Contributions

D.I.H., H.M.A.K., and R.A.E.-S. conceived and design the idea of the current. LC-MS profiling as well as isolation of secondary metabolites using column chromatography were achieved by D.I.H., W.H.B.H., and M.M. In addition, preparative HPLC was carried out by A.M.E. Also, D.I.H., S.S., W.H.B.H., and M.M. elucidated the isolated compounds. The docking study was performed by M.A.N, while the biological experiments were accomplished by H.M.A.K., O.A.A.-F., and R.A.E.-S. Finally, D.I.H., M.M., H.M.A.K., and R.A.E.-S. wrote the original draft. D.I.H., H.M.A.K., R.A.E.-S., W.H.B.H., and S.S. revised the final manuscript, which was agreed by all authors to be published.

Notes

The authors declare no competing financial interest.

■ ABBREVIATIONS USED

^{13}C NMR, carbon-13 nuclear magnetic resonance; 1D NMR, one-dimensional NMR spectroscopy; 2D NMR, two-dimensional NMR spectroscopy; ^{1}H NMR, proton nuclear magnetic resonance; 8OHdG, 8-hydroxy-2′-deoxyguanosine; ATP, adenosine triphosphate; AMP, adenosine monophosphate; ANOVA, analysis of variance; APT, attached proton test; ASP, aspartate; CDK9, cyclin-dependent kinase 9; DMEM, Dulbecco's modified Eagle's medium; DNA, deoxyribonucleic acid; DPPH, 2,2-diphenyl-1-picrylhydrazyl; Drp1, dynamin-related protein 1; EI, electron ionization; ESI-MS, electrospray ionization-mass spectrometry; ET, ethyl acetate; F, fruits; Glu, glutamate; GSH, reduced glutathione; HELA, cervical carcinoma; HepG-2, hepatocellular carcinoma; HIS, histidine; HMBC, heteronuclear multiple bond correlation; IC_{50}, half maximal inhibitory concentration; L, leaves; MDA, malondialdehyde; PHGDH, phosphoglycerate dehydrogenase; S, stems; SAP %, spontaneous alternation percentage; SC_{50} values, concentration required to scavenge the reaction by 50%; Ser, serine; TLC, thin layer chromatography; UPLC-ESI-MS/MS, ultraperformance liquid chromatography-electrospray ionization-tandem mass spectrometry; UV, ultraviolet

https://doi.org/10.1021/acsomega.2c01148
ACS Omega 2022, 7, 16013−16027

REFERENCES

(1) Rahman, A. H. M. M.; Khanom, A. A Taxonomic and Ethno-Medicinal Study of Species from Moraceae (Mulberry) Family in Bangladesh Flora. *Res. Plant Sci.* **2013**, *1* (3), 53−57.

(2) Hussain, F.; Rana, Z.; Shafique, H.; Malik, A.; Hussain, Z. Phytopharmacological Potential of Different Species of Morus Alba and Their Bioactive Phytochemicals: A Review. *Asian Pac. J. Trop. Biomed.* **2017**, *7* (10), 950−956.

(3) Ji, T.; Li, J.; Su, S.-L.; Zhu, Z.-H.; Guo, S.; Qian, D.-W.; Duan, J.-A. Identification and Determination of the Polyhydroxylated Alkaloids Compounds with A-Glucosidase Inhibitor Activity in Mulberry Leaves of Different Origins. *Molecules* **2016**, *21* (2), 206.

(4) Rodrigues, E. L.; Marcelino, G.; Silva, G. T.; Figueiredo, P. S.; Garcez, W. S.; Corsino, J.; Guimarães, R. de C. A.; Freitas, K. de C. Nutraceutical and Medicinal Potential of the Morus Species in Metabolic Dysfunctions. *Int. J. Mol. Sci.* **2019**, *20* (2), 301.

(5) Dai, S.-J.; Ma, Z.-B.; Wu, Y.; Chen, R.-Y.; Yu, D.-Q. Guangsangons F-J, Anti-Oxidant and Anti-Inflammatory Diels-Alder Type Adducts, from Morus Macroura Miq. *Phytochemistry* **2004**, *65* (23), 3135−3141.

(6) Syah, Y. M.; Achmad, S. A.; Ghisalberti, E. L.; Hakim, E. H.; Iman, M. Z. N.; Makmur, L.; Mujahiddin, D. Andalasin A, a New Stilbene Dimer from Morus Macroura. *Fitoterapia* **2000**, *71* (6), 630−635.

(7) Wu, D.-F.; Peng, R.; Ye, L.; Yu, P. The Effects of Silymarin on Hepatic Microsomal and Mitochondrial Membrane Fluidity in Mice. *Zhongguo Zhong Yao Za Zhi* **2003**, *28* (9), 870−872.

(8) Naik, R.; Harmalkar, D. S.; Xu, X.; Jang, K.; Lee, K. Bioactive Benzofuran Derivatives: Moracins A-Z in Medicinal Chemistry. *Eur. J. Med. Chem.* **2015**, *90*, 379−393.

(9) Pilleron, S.; Soto-Perez-de-Celis, E.; Vignat, J.; Ferlay, J.; Soerjomataram, I.; Bray, F.; Sarfati, D. Estimated Global Cancer Incidence in the Oldest Adults in 2018 and Projections to 2050. *Int. J. Cancer* **2021**, *148* (3), 601−608.

(10) Shah, S. C.; Kayamba, V.; Peek, R. M.; Heimburger, D. Cancer Control in Low- and Middle-Income Countries: Is It Time to Consider Screening? *J. Glob. Oncol.* **2019**, *5*, 1−8.

(11) Zhou, W.; Kavelaars, A.; Heijnen, C. J. Metformin Prevents Cisplatin-Induced Cognitive Impairment and Brain Damage in Mice. *PLoS One* **2016**, *11* (3), e0151890.

(12) Vardy, J.; Tannock, I. Cognitive Function after Chemotherapy in Adults with Solid Tumours. *Crit. Rev. Oncol. Hematol.* **2007**, *63* (3), 183−202.

(13) Seigers, R.; Schagen, S. B.; Van Tellingen, O.; Dietrich, J. Chemotherapy-Related Cognitive Dysfunction: Current Animal Studies and Future Directions. *Brain Imaging Behav.* **2013**, *7* (4), 453−459.

(14) Cavaliere, R.; Schiff, D. Neurologic Toxicities of Cancer Therapies. *Curr. Neurol. Neurosci. Rep.* **2006**, *6* (3), 218−226.

(15) Park, S. B.; Krishnan, A. V.; Lin, S. Y.; Goldstein, D.; Friedlander, M.; Kiernan, M. C. Mechanisms Underlying Chemotherapy-Induced Neurotoxicity and the Potential for Neuroprotective Strategies. *Curr. Med. Chem.* **2008**, *15* (29), 3081−94.

(16) Hayati, F.; Hossainzadeh, M.; Shayanpour, S.; Abedi-Gheshlaghi, Z.; Beladi Mousavi, S. Prevention of cisplatin nephrotoxicity. *J. Nephropharmacol.* **2016**, *5* (1), 57−60.

(17) Gomaa, D. H.; Hozayen, W. G.; Al-shafeey Haidy; Hussein Elkelawy, A. M. M.; Hashem, K. S. Ginkgo Biloba Alleviates Cisplatin-Mediated Neurotoxicity in Rats via Modulating APP/Aβ/P2 × 7R/P2Y12R and XIAP/BDNF-Dependent Caspase-3 Apoptotic Pathway. *Appl. Sci.* **2020**, *10* (14), 4786.

(18) Abdel Moneim, A. E. Azadirachta Indica Attenuates Cisplatin-Induced Neurotoxicity in Rats. *Indian J. Pharmacol.* **2014**, *46* (3), 316−321.

(19) Adib Ridzuan, N. R.; Teoh, S. L.; Abdul Rashid, N.; Othman, F.; Baharum, S. N.; Hussan, F. Polygonum minus ethanolic extracts attenuate cisplatin-induced oxidative stress in the cerebral cortex of rats via its antioxidant properties. *Asian Pac. J. Trop. Biomed.* **2019**, *9*, 196−203.

(20) Gomha, S. M.; Riyadh, S. M.; Mahmmoud, E. M.; Elaasser, M. M. Synthesis and anticancer activity of arylazothiazoles and 1, 3, 4-thiadiazoles using chitosan-grafted-poly (4-vinylpyridine) as a novel copolymer basic catalyst. *Chem. Heterocycl. Compd.* **2015**, *51*, 1030−1038.

(21) Halliwell, B. How to Characterize an Antioxidant: An Update. *Biochem. Soc. Symp.* **1995**, *61*, 73−101.

(22) Yen, G. C.; Duh, P. D. Scavenging Effect of Methanolic Extracts of Peanut Hulls on Free-Radical and Active-Oxygen Species. *J. Agric. Food Chem.* **1994**, *42* (3), 629−632.

(23) Owoeye, O.; Adedara, I. A.; Farombi, E. O. Pretreatment with Taurine Prevented Brain Injury and Exploratory Behaviour Associated with Administration of Anticancer Drug Cisplatin in Rats. *Biomed. Pharmacother.* **2018**, *102*, 375−384.

(24) Liu, H. Y.; Fang, M.; Zhang, Y. Q. In Vivo Hypoglycaemic Effect and Inhibitory Mechanism of the Branch Bark Extract of the Mulberry on STZ-Induced Diabetic Mice. *Sci. World J.* **2014**, *2014*, No. e614265.

(25) Hamdan, D. I.; El-Shiekh, R. A.; El-Sayed, M. A.; Khalil, H. M.; Mousa, M. R.; Al-Gendy, A. A.; El-Shazly, A. M. Phytochemical characterization and anti-inflammatory potential of Egyptian Murcott mandarin cultivar waste (stem, leaves and peel). *Food Funct.* **2020**, *11* (9), 8214−8236.

(26) Khalil, H. M. A.; Salama, H. H.; Al-Mokaddem, A. K.; Aljuaydi, S. H.; Edris, A. E. Edible Dairy Formula Fortified with Coconut Oil for Neuroprotection against Aluminium Chloride-Induced Alzheimer's Disease in Rats. *J. Funct. Foods* **2020**, *75*, 104296.

(27) Heinrikson, R. L.; Meredith, S. C. Amino Acid Analysis by Reverse-Phase High-Performance Liquid Chromatography: Precolumn Derivatization with Phenylisothiocyanate. *Anal. Biochem.* **1984**, *136* (1), 65−74.

(28) Pagel, P.; Blome, J.; Wolf, H. U. High-Performance Liquid Chromatographic Separation and Measurement of Various Biogenic Compounds Possibly Involved in the Pathomechanism of Parkinson's Disease. *J. Chromatogr. B. Biomed. Sci. Appl.* **2000**, *746* (2), 297−304.

(29) Jayatilleke, E.; Shaw, S. A High-Performance Liquid Chromatographic Assay for Reduced and Oxidized Glutathione in Biological Samples. *Anal. Biochem.* **1993**, *214* (2), 452−457.

(30) Karatepe, M. Simultaneous determination of ascorbic acid and free malondialdehyde in human serum by HPLC-UV. *LC GC N. Am.* **2004**, *22* (6), 104−106.

(31) Lodovici, M.; Casalini, C.; Briani, C.; Dolara, P. Oxidative Liver DNA Damage in Rats Treated with Pesticide Mixtures. *Toxicology* **1997**, *117* (1), 55−60.

(32) Teerlink, T.; Hennekes, M.; Bussemaker, J.; Groeneveld, J. Simultaneous Determination of Creatine Compounds and Adenine Nucleotides in Myocardial Tissue by High-Performance Liquid Chromatography. *Anal. Biochem.* **1993**, *214* (1), 278−283.

(33) Alberti, A. *LC-ESI-MS/MS methods in profiling of flavonoid glycosides and phenolic acids in traditional medicinal plants: Sempervivum tectorum L. and Corylus avellana L.* Ph.D. Thesis, Semmelweis University, Budapest, Hungary, 2014; DOI: 10.14753/SE.2014.1933.

(34) Kakkar, S.; Bais, S. A Review on Protocatechuic Acid and Its Pharmacological Potential. *ISRN Pharmacol.* **2014**, 952943.

(35) Natic, M. M.; Dabic, D. C.; Papetti, A.; Fotiric Aksic, M. M.; Ognjanov, V.; Ljubojevic, M.; Tesic, Z. Lj. Analysis and Characterisation of Phytochemicals in Mulberry (Morus Alba L.) Fruits Grown in Vojvodina. *Food Chem.* **2015**, *171*, 128−136.

(36) Memon, A. A.; Memon, N.; Luthria, D. L.; Bhanger, M. I.; Pitafi, A. A. Phenolic acids profiling and antioxidant potential of mulberry (Morus laevigata W., Morus nigra L., Morus alba L.) leaves and fruits grown in Pakistan. *Pol. J. Food Nutr. Sci.* **2010**, *60*, 25−32.

(37) Wei, H.; Zhu, J.-J.; Liu, X.-Q.; Feng, W.-H.; Wang, Z.-M.; Yan, L.-H. Review of Bioactive Compounds from Root Barks of Morus Plants (Sang-Bai-Pi) and Their Pharmacological Effects. *Cogent Chem.* **2016**, *2* (1), 1212320.

(38) Plazonić, A.; Bucar, F.; Maleš, Ž.; Mornar, A.; Nigović, B.; Kujundžić, N. Identification and Quantification of Flavonoids and

https://doi.org/10.1021/acsomega.2c01148
ACS Omega 2022, 7, 16013−16027

Phenolic Acids in Burr Parsley (Caucalis Platycarpos L.), Using High-Performance Liquid Chromatography with Diode Array Detection and Electrospray Ionization Mass Spectrometry. *Molecules* **2009**, *14* (7), 2466−2490.
(39) Brito, A.; Ramirez, J. E.; Areche, C.; Sepúlveda, B.; Simirgiotis, M. J. HPLC-UV-MS Profiles of Phenolic Compounds and Antioxidant Activity of Fruits from Three Citrus Species Consumed in Northern Chile. *Molecules* **2014**, *19* (11), 17400−17421.
(40) Doi, K.; Kojima, T.; Makino, M.; Kimura, Y.; Fujimoto, Y. Studies on the Constituents of the Leaves of Morus Alba L. *Chem. Pharm. Bull. (Tokyo)* **2001**, *49* (2), 151−153.
(41) Jing, W.; Yan, R.; Wang, Y. A Practical Strategy for Chemical Profiling of Herbal Medicines Using Ultra-High Performance Liquid Chromatography Coupled with Hybrid Triple Quadrupole-Linear Ion Trap Mass Spectrometry: A Case Study of Mori Cortex. *Anal. Methods* **2015**, *7* (2), 443−457.
(42) Hano, Y.; Nomura, T.; Ueda, S. Two New Diels-Alder Type Adducts, Mulberrofuran T and Kuwanol E, from Callus Tissues of Morus Alba L. *Two New Diels-Alder Type Adducts Mulberrofuran T Kuwanol E Callus Tissues Morus Alba L* **1989**, *29* (10), 2035−2041.
(43) Jin, Q.; Yang, J.; Ma, L.; Cai, J.; Li, J. Comparison of Polyphenol Profile and Inhibitory Activities Against Oxidation and α-Glucosidase in Mulberry (Genus Morus) Cultivars from China. *J. Food Sci.* **2015**, *80* (11), C2440−C2451.
(44) Jin, Q.; Yang, J.; Ma, L.; Wen, D.; Chen, F.; Li, J. Identification of Polyphenols in Mulberry (genus Morus) Cultivars by Liquid Chromatography with Time-of-Flight Mass Spectrometer. *J. Food Compos. Anal.* **2017**, *63*, 55−64.
(45) Kim, W.; Youn, H.; Kang, C.; Youn, B. Inflammation-Induced Radioresistance Is Mediated by ROS-Dependent Inactivation of Protein Phosphatase 1 in Non-Small Cell Lung Cancer Cells. *Apoptosis* **2015**, *20* (9), 1242−1252.
(46) Yang, J.; Liu, X.; Zhang, X.; Jin, Q.; Li, J. Phenolic Profiles, Antioxidant Activities, and Neuroprotective Properties of Mulberry (Morus atropurpurea Roxb.) Fruit Extracts from Different Ripening Stages. *J. Food Sci.* **2016**, *81* (10), C2439−C2446.
(47) Jang, G. H.; Kim, H. W.; Lee, M. K.; Jeong, S. Y.; Bak, A. R.; Lee, D. J.; Kim, J. B. Characterization and Quantification of Flavonoid Glycosides in the Prunus Genus by UPLC-DAD-QTOF/MS. *Saudi J. Biol. Sci.* **2018**, *25* (8), 1622−1631.
(48) Kamalakararao, K.; Rao, D. G.; Muthulingam, M.; Gopalakrishnan, V. K.; Hagos, Z.; Dogulas, P. J.; Chaithanya, K. K. Effect of Isolated Bioactive Flavonoid Apigenin-7-O-B-D-Glucuronide Methyl Ester on Cyclooxygenase-2 Gene Expression in the Breast Cancer MCF-7 Cell Lines. *Drug Invent. Today* **2018**, *10*, 3552−3555.
(49) Ibrahim, R. M.; El-Halawany, A. M.; Saleh, D. O.; El Naggar, E. M. B.; El-Shabrawy, A. E.-R. O.; El-Hawary, S. S. HPLC-DAD-MS/MS Profiling of Phenolics from Securigera Securidaca Flowers and Its Anti-Hyperglycemic and Anti-Hyperlipidemic Activities. *Rev. Bras. Farmacogn.* **2015**, *25* (2), 134−141.
(50) Simirgiotis, M. J.; Bórquez, J.; Schmeda-Hirschmann, G. Antioxidant Capacity, Polyphenolic Content and Tandem HPLC-DAD-ESI/MS Profiling of Phenolic Compounds from the South American Berries Luma Apiculata and L. Chequén. *Food Chem.* **2013**, *139* (1), 289−299.
(51) Tallini, L. R.; Pedrazza, G. P.R.; Bordignon, S. A. d. L.; Costa, A. C.O.; Steppe, M.; Fuentefria, A.; Zuanazzi, J. A.S. Analysis of Flavonoids in Rubus Erythrocladus and Morus Nigra Leaves Extracts by Liquid Chromatography and Capillary Electrophoresis. *Rev. Bras. Farmacogn.* **2015**, *25* (3), 219−227.
(52) Wang, Y.; Yang, M.-H.; Wang, X.-B.; Li, T.-X.; Kong, L.-Y. Bioactive Metabolites from the Endophytic Fungus Alternaria Alternata. *Fitoterapia* **2014**, *99*, 153−158.
(53) Manthey, J. HPLC-MS Analysis of Coumarins and Furanocoumarin Dimers in Immature Grapefruit. *Proc. Fla. State Hortic. Soc.* **2005**, *118*, 429−436.
(54) Lim, T. K. *Edible Medicinal and Non-Medicinal Plants*; Springer, 2012.
(55) Yang, N. Y.; Yang, Y. F.; Li, K. Analysis of Hydroxy Fatty Acids from the Pollen of Brassica campestris L. var. oleifera DC. by UPLC-MS/MS. *J. Pharm.* **2013**, *2013*, 874875.
(56) Kay, C. D.; Mazza, G.; Holub, B. J.; Wang, J. Anthocyanin Metabolites in Human Urine and Serum. *Br. J. Nutr.* **2004**, *91* (6), 933−942.
(57) Fongang, Y. S. F.; Bankeu, J. J. K.; Ali, M. S.; Awantu, A. F.; Zeeshan, A.; Assob, C. N.; Mehreen, L.; Lenta, B. N.; Ngouela, S. A.; Tsamo, E. Flavonoids and Other Bioactive Constituents from Ficus Thonningii Blume (Moraceae). *Phytochem. Lett.* **2015**, *11*, 139−145.
(58) Sun, Y.; Yang, T.; Leak, R. K.; Chen, J.; Zhang, F. Preventive and Protective Roles of Dietary Nrf2 Activators against Central Nervous System Diseases. *CNS Neurol. Disord. Drug Targets* **2017**, *16* (3), 326−338.
(59) Suttiarporn, P.; Chumpolsri, W.; Mahatheeranont, S.; Luangkamin, S.; Teepsawang, S.; Leardkamolkarn, V. Structures of Phytosterols and Triterpenoids with Potential Anti-Cancer Activity in Bran of Black Non-Glutinous Rice. *Nutrients* **2015**, *7* (3), 1672−1687.
(60) Silvestro, L.; Tarcomnicu, I.; Dulea, C.; Attili, N. R. B. N.; Ciuca, V.; Peru, D.; Rizea Savu, S. Confirmation of Diosmetin 3-O-Glucuronide as Major Metabolite of Diosmin in Humans, Using Micro-Liquid-Chromatography-mass Spectrometry and Ion Mobility Mass Spectrometry. *Anal. Bioanal. Chem.* **2013**, *405* (25), 8295−8310.
(61) Ali, A.; Jameel, M.; Ali, M. Fatty Acids Analysis of Ficus Religiosa Stem Bark by Gas Chromatography-Mass Spectrometry. *Int. J. Adv. Pharm. Med. Bioallied Sci.* **2017**, *2017*, 112.
(62) Silva, A. T. M. e; Magalhaes, C. G.; Duarte, L. P.; Mussel, W. d. N.; Ruiz, A. L. T. G.; Shiozawa, L.; Carvalho, J. E. d.; Trindade, I. C.; Vieira Filho, S. A. Lupeol and its esters: NMR, powder XRD data and in vitro evaluation of cancer cell growth. *Braz. J. Pharm. Sci.* **2018**, *53* (3), e00251.
(63) Decendit, A.; Mamani-Matsuda, M.; Aumont, V.; Waffo-Teguo, P.; Moynet, D.; Boniface, K.; Richard, E.; Krisa, S.; Rambert, J.; Mérillon, J.-M.; Mossalayi, M. D. Malvidin-3-O-B Glucoside, Major Grape Anthocyanin, Inhibits Human Macrophage-Derived Inflammatory Mediators and Decreases Clinical Scores in Arthritic Rats. *Biochem. Pharmacol.* **2013**, *86* (10), 1461−1467.
(64) Jameel, M.; Ali, A.; Ali, M. Identification of New Compounds from Fumaria Parviflora Lam. -. *J. Appl. Pharm. Sci.* **2017**, *7* (04), 053−060.
(65) Hassimotto, N. M. A.; Genovese, M. I.; Lajolo, F. M. Identification and Characterisation of Anthocyanins from Wild Mulberry (Morus Nigra L.) Growing in Brazil. *Food Sci. Technol. Int.* **2007**, *13* (1), 17−25.
(66) Sastry, V. M. V. S.; Rao, G. R. K. Dioctyl Phthalate, and Antibacterial Compound from the Marine Brown Alga —Sargassum Wightii. *J. Appl. Phycol.* **1995**, *7* (2), 185−186.
(67) Szajdek, A.; Borowska, E. J. Bioactive Compounds and Health-Promoting Properties of Berry Fruits: A Review. *Plant Foods Hum. Nutr.* **2008**, *63* (4), 147−156.
(68) Mazzuca, P.; Ferranti, P.; Picariello, G.; Chianese, L.; Addeo, F. Mass Spectrometry in the Study of Anthocyanins and Their Derivatives: Differentiation of Vitis Vinifera and Hybrid Grapes by Liquid Chromatography/electrospray Ionization Mass Spectrometry and Tandem Mass Spectrometry. *J. Mass Spectrom.* **2005**, *40* (1), 83−90.
(69) Gouvêa, A. C. M. S.; Araujo, M. C. P. de; Schulz, D. F.; Pacheco, S.; Godoy, R. L. de O.; Cabral, L. M. C. Anthocyanins Standards (cyanidin-3-O-Glucoside and Cyanidin-3-O-Rutinoside) Isolation from Freeze-Dried Açaí (Euterpe Oleraceae Mart.) by HPLC. *Food Sci. Technol.* **2012**, *32* (1), 43−46.
(70) Gecgel, U.; Velioglu, S. D.; Velioglu, H. M. Investigating Some Physicochemical Properties and Fatty Acid Composition of Native Black Mulberry (Morus Nigra L.) Seed Oil. *J. Am. Oil Chem. Soc.* **2011**, *88* (8), 1179−1187.
(71) Zhang, Q.-J.; Tang, Y.-B.; Chen, R.-Y.; Yu, D.-Q. Three New Cytotoxic Diels-Alder-Type Adducts from Morus Australis. *Chem. Biodivers.* **2007**, *4* (7), 1533−1540.

https://doi.org/10.1021/acsomega.2c01148
ACS Omega 2022, 7, 16013−16027

(72) Sánchez-Salcedo, E. M.; Sendra, E.; Carbonell-Barrachina, Á. A.; Martínez, J. J.; Hernández, F. Fatty Acids Composition of Spanish Black (Morus Nigra L.) and White (Morus Alba L.) Mulberries. *Food Chem.* **2016**, *190*, 566−571.
(73) Im, S. H.; Wang, Z.; Lim, S. S.; Lee, O.-H.; Kang, I.-J. Bioactivity-Guided Isolation and Identification of Anti-Adipogenic Compounds from Sanguisorba Officinalis. *Pharm. Biol.* **2017**, *55* (1), 2057−2064.
(74) Zhang, H.; Ma, Z. F.; Luo, X.; Li, X. Effects of Mulberry Fruit (Morus alba L.) Consumption on Health Outcomes: A Mini-Review. *Antioxidants* **2018**, *7* (5), 69.
(75) Miljkovic, V.; Nikolic, L.; Radulovic, N.; Arsic, B.; Nikolic, G.; Kostic, D.; Zvezdanovic, J.; Bojanic, Z. Flavonoids from Mulberry Fruit (Morus alba L., Morus rubra L. and Morus nigra L.). *Agro Food Industry Hi Tech* **2015**, *26* (3), 38−42.
(76) Ferlinahayati, F.; Syah, Y. M.; Juliawaty, L. D.; Hakim, E. H. Flavanones from the Wood of Morus Nigra with Cytotoxic Activity. *Indones. J. Chem.* **2013**, *13* (3), 205−208.
(77) Schütz, K.; Persike, M.; Carle, R.; Schieber, A. Characterization and Quantification of Anthocyanins in Selected Artichoke (Cynara Scolymus L.) Cultivars by HPLC-DAD-ESI-MSn. *Anal. Bioanal. Chem.* **2006**, *384* (7), 1511−1517.
(78) Sánchez-Salcedo, E. M.; Mena, P.; García-Viguera, C.; Hernández, F.; Martínez, J. J. (Poly) phenolic compounds and antioxidant activity of white (Morus alba) and black (Morus nigra) mulberry leaves: Their potential for new products rich in phytochemicals. *J. Funct. Foods* **2015**, *18*, 1039−1046.
(79) Srisawat, T.; Chumkaew, P.; Heed-Chim, W.; Sukpondma, Y.; Kanokwiroon, K. Phytochemical Screening and Cytotoxicity of Crude Extracts of Vatica Diospyroides Symington Type LS. *Trop. J. Pharm. Res.* **2013**, *12* (1), 71−76.
(80) Rahman, K. Studies on Free Radicals, Antioxidants, and Co-Factors. *Clin. Interv. Aging* **2007**, *2* (2), 219−236.
(81) Chiu, G. S.; Maj, M. A.; Rizvi, S.; Dantzer, R.; Vichaya, E. G.; Laumet, G.; Kavelaars, A.; Heijnen, C. J. Pifithrin-M Prevents Cisplatin-Induced Chemobrain by Preserving Neuronal Mitochondrial Function. *Cancer Res.* **2017**, *77* (3), 742−752.
(82) Ma, J.; Huo, X.; Jarpe, M. B.; Kavelaars, A.; Heijnen, C. J. Pharmacological Inhibition of HDAC6 Reverses Cognitive Impairment and Tau Pathology as a Result of Cisplatin Treatment. *Acta Neuropathol. Commun.* **2018**, *6* (1), 103.
(83) Lee, B.; Yeom, M.; Shim, I.; Lee, H.; Hahm, D. H. Protective Effects of Quercetin on Anxiety-Like Symptoms and Neuroinflammation Induced by Lipopolysaccharide in Rats. *Evid. Based Complement. Alternat. Med.* **2020**, *2020*, 4892415.
(84) Ahmad, H.; Rauf, K.; Zada, W.; McCarthy, M.; Abbas, G.; Anwar, F.; Shah, A. J. Kaempferol Facilitated Extinction Learning in Contextual Fear Conditioned Rats via Inhibition of Fatty-Acid Amide Hydrolase. *Molecules* **2020**, *25* (20), 4683.
(85) Dauvermann, M. R.; Lee, G.; Dawson, N. Glutamatergic Regulation of Cognition and Functional Brain Connectivity: Insights from Pharmacological, Genetic and Translational Schizophrenia Research. *Br. J. Pharmacol.* **2017**, *174* (19), 3136−3160.
(86) Zhou, Y.; Danbolt, N. C. Glutamate as a Neurotransmitter in the Healthy Brain. *J. Neural Transm.* **2014**, *121* (8), 799−817.
(87) Farber, J. L. The Role of Calcium Ions in Toxic Cell Injury. *Environ. Health Perspect.* **1990**, *84*, 107−111.
(88) Kritis, A. A.; Stamoula, E. G.; Paniskaki, K. A.; Vavilis, T. D. Researching glutamate - induced cytotoxicity in different cell lines: a comparative/collective analysis/study. *Front. Cell. Neurosci.* **2015**, *9*, 91.
(89) Lewerenz, J.; Hewett, S. J.; Huang, Y.; Lambros, M.; Gout, P. W.; Kalivas, P. W.; Massie, A.; Smolders, I.; Methner, A.; Pergande, M.; Smith, S. B.; Ganapathy, V.; Maher, P. The Cystine/Glutamate Antiporter System Xc- in Health and Disease: From Molecular Mechanisms to Novel Therapeutic Opportunities. *Antioxid. Redox Signal.* **2013**, *18* (5), 522−555.
(90) Imran, M.; Salehi, B.; Sharifi-Rad, J.; Aslam Gondal, T.; Saeed, F.; Imran, A.; Shahbaz, M.; Tsouh Fokou, P. V.; Umair Arshad, M.; Khan, H.; Guerreiro, S. G.; Martins, N.; Estevinho, L. M. Kaempferol: A Key Emphasis to Its Anticancer Potential. *Molecules* **2019**, *24* (12), 2277.
(91) Vellosa, J. C. R.; Regasini, L. O.; Khalil, N. M.; Bolzani, V. da S.; Khalil, O. A. K.; Manente, F. A.; Pasquini Netto, H.; Oliveira, O. M. M. de F. Antioxidant and Cytotoxic Studies for Kaempferol, Quercetin and Isoquercitrin. *Eclética Quím.* **2011**, *36* (2), 07−20.
(92) Green, D. R.; Galluzzi, L.; Kroemer, G. Metabolic control of cell death. *Science* **2014**, *345* (6203), 1250256.
(93) Kim, J.-H.; Kim, Y.-S.; Song, G.-G.; Park, J.-J.; Chang, H.-I. Protective Effect of Astaxanthin on Naproxen-Induced Gastric Antral Ulceration in Rats. *Eur. J. Pharmacol.* **2005**, *514* (1), 53−59.
(94) Silva dos Santos, J.; Gonçalves Cirino, J. P.; de Oliveira Carvalho, P.; Ortega, M. M. The Pharmacological Action of Kaempferol in Central Nervous System Diseases: A Review. *Front. Pharmacol.* **2021**, *13* (11), 2143.
(95) Panula, P.; Nuutinen, S. The Histaminergic Network in the Brain: Basic Organization and Role in Disease. *Nat. Rev. Neurosci.* **2013**, *14* (7), 472−487.
(96) Jafarinia, M.; Sadat Hosseini, M.; kasiri, N.; Fazel, N.; Fathi, F.; Ganjalikhani Hakemi, M.; Eskandari, N. Quercetin with the Potential Effect on Allergic Diseases. *Allergy Asthma Clin. Immunol.* **2020**, *16* (1), 1−11.
(97) Hosios, A. M.; Hecht, V. C.; Danai, L. V.; Johnson, M. O.; Rathmell, J. C.; Steinhauser, M. L.; Manalis, S. R.; Vander Heiden, M. G. Amino Acids Rather than Glucose Account for the Majority of Cell Mass in Proliferating Mammalian Cells. *Dev. Cell* **2016**, *36* (5), 540−549.
(98) Zhao, X.; Fu, J.; Tang, W.; Yu, L.; Xu, W. Inhibition of Serine Metabolism Promotes Resistance to Cisplatin in Gastric Cancer. *OncoTargets Ther.* **2020**, *13*, 4833−4842.
(99) Chen, C.; Huang, J.; Shen, J.; Bai, Q. Quercetin Improves Endothelial Insulin Sensitivity in Obese Mice by Inhibiting Drp1 Phosphorylation at Serine 616 and Mitochondrial Fragmentation. *Acta Biochim. Biophys. Sin.* **2019**, *51* (12), 1250−1257.

https://doi.org/10.1021/acsomega.2c01148
ACS Omega 2022, 7, 16013−16027